1-7-2007

Application of H-, P- and HP-Adaptation for Convective Heat Transfer Problems

Xiuling Wang
University of Nevada, Las Vegas

Darrell W. Pepper
University of Nevada, Las Vegas, darrell.pepper@unlv.edu

45th AIAA Aerospace Sciences Meeting and Exhibit
8 - 11 January 2007, Reno, Nevada

AIAA 2007-803

Application of *h*-, *p*- and *hp*-adaptation for Convective Heat Transfer Problems

Xiuling Wang* and Darrell W. Pepper†

4505 Maryland Parkway, Box 454027, Las Vegas, NV 89154-4027

Simulation results using three well-known adaptive finite element algorithms to solve convective heat transfer are presented. The algorithms are: *h*-adaptation (based on mesh refinement); *p*-adaptation (based on mesh enrichment); and *hp*-adaptation (based on both mesh refinement and enrichment). The adaptation procedures are controlled by an *a posterior error* estimator based on L_2 norm calculation. Natural convection in a differentially heated square cavity is first solved using the algorithms; the three schemes are then applied to natural convective heat transfer within a partitioned enclosure. Results are compared with data available in literature for both cases.

Nomenclature

A	Advection matrix
B	Body force
F_T	Load vector for temperature
F_V	Load vector for velocity
h_e	Characteristic element length
h	Element size
K_T	Diffusion matrix for temperature
K_V	Diffusion matrix for velocity
m	Total element number
M	Mass matrix
N_i	Shape function
p	Shape function order, pressure
t	Time
$\mathrm{P_r}$	Prandtl number
P_e	Peclet number
R_a	Rayleigh number
$\mathrm{R_e}$	Reynolds number
V	Velocity vector
W_i	Petrov-Garlerkin weighted function
x	Dimensional space (x, y)
α	Thermal diffusivity, Petrov-Galerkin weighting factor
β	Thermal expansion coefficient
γ	Petrov-Galerkin stability parameter
Ω	Computational domain

* Research Assistant Professor, NCACM, University of Nevada, Las Vegas 89154, AIAA Member
† Professor and Director, NCACM, Department of Mechanical Engineering, University of Nevada, Las Vegas; AIAA Associate Fellow

∇ Divergence operator
$\nabla\bullet$ Dot product

1. Introduction

The finite element method (FEM) is now being widely used in solving fluid and thermal flow problems. Adaptive FEM is becoming especially attractive as it can dynamically control the element size and shape function order according to error distributions. Large errors are usually associated with locations where flow features change rapidly - thus fine mesh or higher order shape function are commonly adopted. Small errors are usually associated with smooth flow regions, where coarse mesh or lower order shape function are adopted.

Generally, four categories of adaptation exist: (1) *h*-adaptation, where the element sizes vary while the order of the shape functions are constant; (2) *p*-adaptation, where the element sizes are constant while the order of the shape functions increase to meet desired accuracy requirements; (3) *r*-adaptation, where the nodes are redistributed in an existing mesh in the process of adaptation; (4) *hp*-adaptation, which is the combination of both *h*-and *p*-adaptation. *hp*-adaptive schemes are among the best mesh-based schemes with the potential payoff of obtaining exponential convergence rates [1, 2].

In this study, three adaptive FEM algorithms are employed to solve incompressible flows with heat transfer effects: natural convection in a differentially heated cavity and natural convection within a partitioned enclosure. Simulation results agree well with data in the literature. Computational accuracies, efficiencies, and requirements of the three adaptive FEM algorithms are compared and discussed.

2. Governing Equations

The non-dimensional governing equations for incompressible, laminar Boussinesq flow for natural convective heat transfer can be written as [3]

Continuity equation:

$$\nabla\bullet V = 0 \tag{1}$$

Momentum equation:

$$\frac{\partial V}{\partial t} + V\bullet\nabla V = -\nabla p + \Pr\nabla^2 V + C_{grav}T \tag{2}$$

Energy equation:

$$\frac{\partial T}{\partial t} + V\bullet\nabla T = \nabla^2 T \tag{3}$$

where in x-dir, $C_{grav} = 0$; in y-dir, $C_{grav} = Ra\Pr$.

3. Finite Element Formulations and Solution Procedure

Quadrilateral elements are used to discretize two-dimensional problem domains; hexahedral elements are employed for three-dimensional problems. The Galerkin weighted residual method is used.

The variables V and T are replaced with the trial functions

$$V(x,t) = \sum_{i=1}^{n} N_i(x)V_i(t) \qquad T(x,t) = \sum_{i=1}^{n} N_i(x)T_i(t) \tag{4}$$

where x is the computational domain, i is the degree of freedom (DOF) index and n is the number of DOFs.

A projection method is used as the flow solver. This method is based on the Helmholtz-Hodge Decomposition Theorem (Chorin et al. [4]), and detailed description of employment of projection method can be found in the work of Ramaswamy et al. [5].

Under projection algorithms, the weighted residual forms of the momentum and energy equations can be written as (summation convention is implied)

Momentum:

$$\left(\int_\Omega N_i N_j d\Omega\right)\left\{\dot{V}_i\right\}+\left(\int_\Omega N_i\left(N_k V_k\right)\frac{\partial N_j}{\partial x_j}d\Omega\right)\left\{V_i\right\}+\left(\int_\Omega \Pr\frac{\partial N_i}{\partial x_i}\frac{\partial N_j}{\partial x_j}d\Omega\right)\left\{V_i\right\}$$
$$-\int_\Omega f\left(x_i\right)N_i d\Omega-\int_\Omega \Pr N_i\frac{\partial N_j}{\partial x_j}\left\{V_i\right\}n_i d\Gamma=0 \tag{5}$$

where Ω denotes (**x**) and Γ represents the boundaries of the computational domain. For the vertical component (y) with natural convective effects: $f\left(x_i\right)=C_{grav}\left\{T_i\right\}=Ra\Pr\left\{T_i\right\}$

Energy:

$$\left(\int_\Omega N_i N_j d\Omega\right)\left\{\dot{T}_i\right\}+\left(\int_\Omega N_i\left(N_k V_k\right)\frac{\partial N_j}{\partial x_j}d\Omega\right)\left\{T_i\right\}+\left(\int_\Omega \frac{\partial N_i}{\partial x_i}\frac{\partial N_j}{\partial x_j}d\Omega\right)\left\{T_i\right\}$$
$$-\int_\Omega QN_i d\Omega-\int_\Omega N_i q\Gamma d\Gamma=0 \tag{6}$$

Equations (8) and (9) can be written in matrix form as

$$[\mathrm{M}]\{\dot{\mathrm{V}}\}+([\mathrm{K_V}]+[\mathrm{A(V)}])\{\mathrm{V}\}=\{\mathrm{F_V}\} \tag{7}$$

$$[\mathrm{M}]\{\dot{\mathrm{T}}\}+([\mathrm{K_T}]+[\mathrm{A(V)}])\{\mathrm{T}\}=\{\mathrm{F_T}\} \tag{8}$$

where the over dot refers to time differentiation. Detailed descriptions of the matrix coefficients are given in [3].

4. Adaptation Techniques

In order to employ adaptation techniques successfully, certain rules must be followed. Other key issues that need to be considered include error estimator and adaptation strategies. Some of the more important adaptation rules, error estimators and adaptation strategies are stated in the following sections. Details are discussed in [1, 2] and [6-11].

4.1. Adaptation rules

In *h*-adaptation, 1-irregular mesh adaptation rule can avoid multiple constrained nodes (parent node themselves are constraint nodes): an element can be refined only if its neighbors are at the same or higher level (1-irregular mesh), an element can be unrefined only if its neighbors are at the same or lower level (1-irregular mesh).

In *p*-adaptation, hierarchical shape functions are employed. When an element is enriched, because of the characteristic of hierarchical shape functions, all the element matrices and previous computational information relating to that element does not need to be discard, not necessary to recalculate of the stiffnesses and load vectors either. The hierarchical shape functions employed in *p*-adaptation can be categorized as: node functions, edge functions, face functions (for 3D cases) and bubble functions. Minimum rule need to be followed in *p*-adaptation: the order for an edge common for two elements never exceeds orders of the neighboring middle nodes. For quadrilateral elements in 2D, both the horizontal and vertical orders must be considered.

As a combination of *h*- and *p*- adaptation, *hp*-adaptation can be either refined (unrefined) or enriched (unenriched) whenever necessary. The adaptation rules for *h*- and *p*- are combined in *hp*-adaptation. In addition, to maintain continuity of global basis function, constraints at the interface of elements supporting edge functions of different order are employed. The constraint represents a generalization of the *hp*-constraints, which is discussed in detail by Demkowicz et al [6].

4.2. Error estimator

Various error estimators exist that can be used in adaptation, e.g., the element residual method, interpolation methods, subdomain-residual methods, and projection method. Selection of a good error estimator is fundamental to employing a successful adaptation procedure. Detailed descriptions of different error estimators can be found in [7]-[10].

In this study, an error estimator was chosen based on an extension of the work by Zienkiewicz and Zhu [8] due to its reasonable accuracy, simplicity and ease of implementation. The errors in a finite element solution are the differences between the exact and approximate solutions, which can be expressed in certain norms such as the "energy" norm or L_2 norm. In this simulation, the L_2 norm is adopted [3]. Temperature is chosen as the key adaptation variable in this study.

4.3. Adaptation strategy

Two conditions are required to be met for an acceptable solution: global error and local error. A global error condition states that the global percentage error should not be greater than a maximum specified percentage error: $\eta \le \overline{\eta}_{\max}$. If $\eta > \overline{\eta}_{\max}$, a new iteration is performed. The local error condition states that local relative percentage error of any single element $\|e_\sigma\|_i$ should not be greater than the averaged error $\overline{e}_{avg}$ among all the elements in the domain.

In an *h*-adaptive process, the new element size is calculated using:

$$h_{new} = \frac{h_{old}}{\xi_i^{1/p}} \tag{9}$$

In a *p*-adaptive process, the new shape function order is calculated using:

$$p_{new} = p_{old}\xi_i^{1/p} \tag{10}$$

The *hp*-adaptive strategy used in this study employs a "L_2" norm error estimator, which is an extension from the "three-step *hp*-adaptive strategy" developed by Oden et al [11]. In the *hp*-adaptive procedure, a sequence of refinement steps is employed. Three consecutive *hp*-adaptive meshes are constructed for solving the system in order to reach a preset target error: initial mesh, the intermediate *h*-adaptive mesh, and the final *hp*- adaptive mesh obtained by applying *p*-adaptive enrichments on the intermediate mesh. The *p*-adaptation is carried out when the problem solution is pre-asymptotic.

5. Natural Convection in a Square Enclosure

Natural convection in a square enclosure has been studied extensively over the past 40 years. Many engineering problems of practical interest deal with buoyant flows in enclosures, such as thermal insulation of buildings, heat transfer inside attic, cooling of nuclear reactor cores, etc (Pelletier [12]). De Vahl Davis [13] provided accurate benchmark solutions for natural convection in a square enclosure, using a finite difference method with a stream function and vorticity formulations for solving this problem.

A nondimensional enclosure with dimensions $0 \le x \le 1, 0 \le y \le 1$ is heated on the left wall and cooled on the right wall; the top and bottom walls are insulated. The Prandtl number is Pr = 0.71 and Ra = 10^3-10^5.

Steady state results were obtained for Ra = 10^3 – 10^5. Excellent agreement was observed over the range of Ra numbers with data available in the literature [13]. Results from the lower Ra number computations are essentially duplicative with results found in the literature. Results for Ra =10^5 are presented in this paper. Final adapted meshes resulted in 2503 elements and 2542 DOFs (degrees of freedom) in *h*-adaptation; 400 elements and 1184 DOFs in *p*-adaptation; and 1368 elements and 6894 DOFs in *hp*-adaptation. The final adapted meshes are shown in Figure 1.

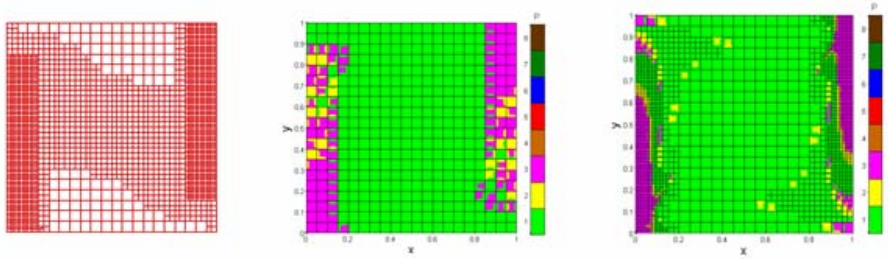

(a) (b) (c)

Figure 1. Final adaptive meshes (a) *h*-adaptation (b) *p*-adaptation and (c) *hp*-adaptation

Simulation results for streamfunction and temperature contours are presented. All the adaptive results agree well with benchmark data available for both flow and thermal patterns [13]. Figure 2 shows streamfunction contours (-9.507 and -8.646 to 0 in 0.9607 intervals). Figure 3 shows isotherms (contours vary from 0 to 1 in 0.1 intervals).

(a) (b) (c)

Figure 2. Streamfunction contours (a) *h*-adaptation (b) *p*-adaptation and (c) *hp*-adaptation

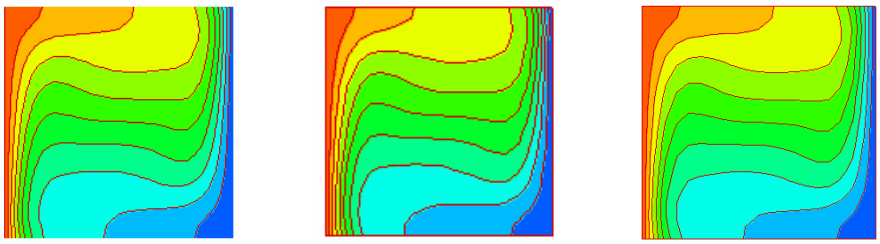

(a) (b) (c)

Figure 3. Temperature contours (a) *h*-adaptation (b) *p*-adaptation and (c) *hp*-adaptation

Error distributions are shown in Figure 4. Compare the three adaptive algorithms, *hp*-adaptive algorithm has the most equally distributed error, which again demonstrates *hp*-adaptive algorithm is one of the best mesh based schemes.

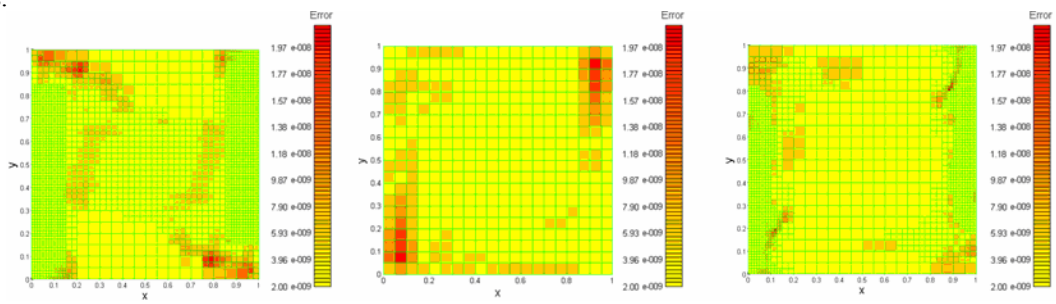

(a) (b) (c)

Figure 4. Error Distributions (a) *h*-adaptation (b) *p*-adaptation and (c) *hp*-adaptation

Quantitative studies were also conducted for the adaptive algorithms with $Ra=10^5$. Comparisons with [13] were made for the maximum horizontal and vertical velocities together with their locations on the vertical and horizontal midplane; Nu_0, the average Nusselt number on the heated wall; and the maximum and minimum values of local Nusselt number on the heated side together with their locations. Comparison values are shown in Table 1.

Table 1. Comparison of *hp*-FEM results with benchmark data ($Ra=10^5$)

	[13] results	*h*-FEM results	*p*-FEM results	*hp*-FEM results
u_{max}	34.73	34.87	34.89	34.85
y (x=0.5)	0.855	0.865	0.865	0.864
v_{max}	68.59	68.71	68.69	68.67
x (y=0.5)	0.066	0.074	0.073	0.070
Nu_0	4.509	4.513	4.516	4.511
Nu_{max}	7.717	7.725	7.727	7.720
y (x=0)	0.081	0.085	0.088	0.084
Nu_{min}	0.729	0.736	0.738	0.731
y (x=0)	1	1	1	1

6. Natural Convection in an Enclosed Partition

Free convection heat transfer within an enclosed partition has many engineering applications such as fire spread and energy transfer in rooms and buildings, cooling of nuclear reactors, heat transfer across thermo pane windows, it is also related to heat exchanger design [14, 15]. This geometry also corresponds to a printed circuit, or a ceiling beam in a room.

The partitioned enclosure is defined as $0 \le x \le L, 0 \le y \le L$; the partition thickness is $0.1L$, the height for the partition is $H = 0.3L$, and the location of the partition departing from the hot wall is $d = 0.7L$. The configuration of the partitioned enclosure is shown in Figure 5. The left wall is hot and the right wall is cold; walls along with the top, bottom and the partition are insulated.

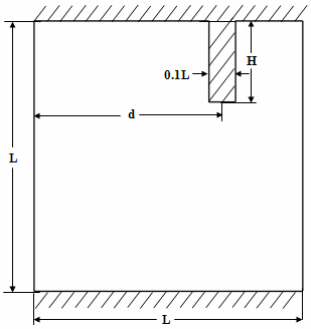

Figure 5. Partial divided enclosure

Steady state results for Pr = 0.71 and Ra = 10^4 are presented. The final adapted meshes resulted in 2059 elements and 2081 DOFs (degree of freedoms) in *h*-adaptation; 388 elements and 2449 DOFs in *p*-adaptation; and 1261 elements and 4714 DOFs in *hp*-adaptation. The final adaptive meshes are shown in Figure 6.

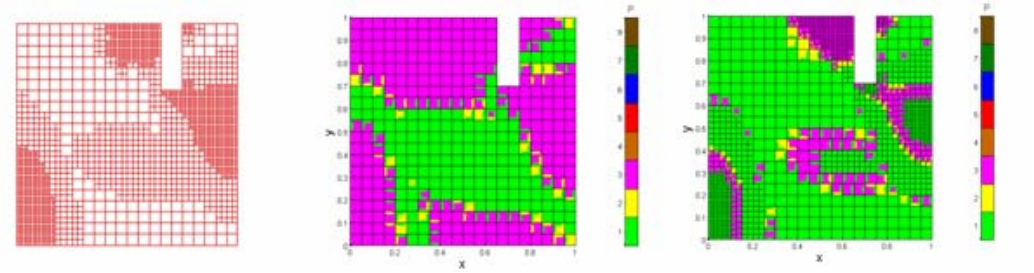

(a) (b) (c)

Figure 6. Final adaptive meshes (a) *h*-adaptation (b) *p*-adaptation and (c) *hp*-adaptation

Simulation results for streamfunction and temperature contours are presented. All the adaptive results agree well with benchmark data available in the literature for both flow and thermal patterns [15]. Figure 7 shows streamfunction contours (-3.282 to 0 in 0.328 intervals) while isotherms (contours vary from 0 to 1 in 0.1 intervals) are shown in Figure 8.

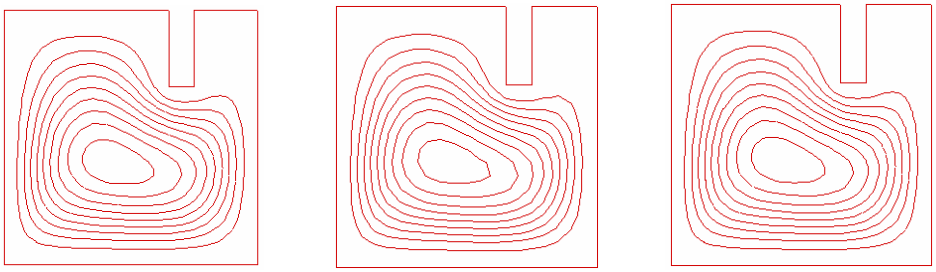

(a) (b) (c)

Figure 7. Streamfunction contours (a) *h*-adaptation (b) *p*-adaptation and (c) *hp*-adaptation

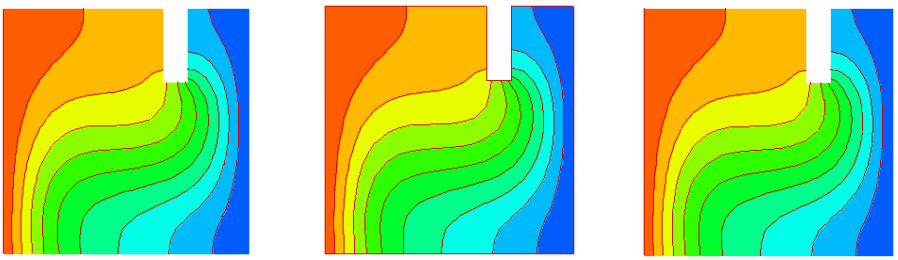

(a) (b) (c)

Figure 8. Temperature contours (a) *h*-adaptation (b) *p*-adaptation and (c) *hp*-adaptation

7. Discussion

In this paper, three adaptive algorithms were developed. The element size (*h*-adaptation), the shape function order (*p*-adaptation), or both (*hp*-adaptation) are dynamically controlled in the adaptation procedure based on error distribution. Meshes are generally clustered (or higher order shape function are adopted) in the boundary layers (see Figure 1 and 5, along vertical boundary layer), or in flow accelerated regions (see Figure 5, around partition corners). Because of the rapidly changing flow and thermal conditions in those regions, large errors are produced – this ultimately results in either finer local mesh or higher order shape functions, or both, adapted to reach desired accuracy.

All three adaptive algorithms are cost efficient in reducing overall computational time and achieving accurate solutions. This is particularly true when one compares *h*-adaptation with a uniformly refined algorithm, *p*-adaptation is compared with a uniformly enriched algorithm, and *hp*-adaptation is compared with a uniformly refined and enriched algorithm. Comparisons of CPU time using the adaptive algorithms for the first test case are shown in Table 2. Results showed that a globally *h*-refined algorithm consumed nearly 1.4X more CPU/DOF than the *h*-adaptive algorithm; a globally *p*-enriched algorithm consumed almost 1.5X more CPU/DOF than the *p*-adaptive algorithm; a globally *h*-refined and *p*-enriched algorithm consumed almost 1.7X more CPU/DOF (projected) than the *hp*-adaptive algorithm. Even though the CPU/DOF time is the smallest for the *p*-adaptive algorithm for this simple problem, the error convergence of the *hp*-adaptive technique is still superior to both the *h*- and the *p*-adaptive schemes [1, 2]; this can be seen in Fig. 4.

Table 2. CPU time comparison between uniform refined and enriched algorithm and *hp*-adaptive algorithm

Compare Cases	# of elements Initial	Final	# of DOF Initial	Final	CPU/DOF (sec/DOF)
Uniform *h* and *p*	6,400	6,400	58,081	58,081	9.85
hp-adaptive algorithm	400	1,368	441	6,894	5.66
Uniform *h*	6,400	6,400	6,561	6,561	8.42
h- adaptive algorithm	400	2,503	441	2,542	5.89
Uniform *p*	400	400	441	3,721	7.21
p- adaptive algorithm	400	400	441	1,184	4.66

Of the three adaptive algorithms, *hp*-adaptation is generally the preferred choice. However, different adaptive algorithms have their own advantages and disadvantages, which are summarized in Table 3. The decision of choosing which particular type of adaptive algorithm and which variable as the key parameter to control depends on various problem constraints and properties desired by the user. For example, a simple rectangular domain with simple boundary condition constraints can be solved without adaptation using conventional numerical methods. On the other hand, complex geometries and regions where high gradients develop are best handled using dynamic adaptive techniques – and eliminate the burden on the user of having to remesh the problem. In some calculations

where it becomes difficult in predicting the flow and thermal features, dynamically controlled adaptive algorithms can provide an efficient way to reach desired accuracy.

Table 3. Comparison of *h*-, *p*-, *r*- and *hp*- adaptive algorithm

	h-adaptation	*p*-adaptation	*r*-adaptation	*hp*-adaptation
element size	various	constant	various	various
DOF (degrees of freedom)	various	various	constant	various
shape function	constant	various	constant	various
advantages	elements will not become overly distorted	relative coarse mesh may be sufficient	no new nodes added	exponential convergence rate
disadvantages	difficulty in dealing with constraint nodes	coding complexity	elements may become overly distorted	difficulty in dealing with constraint nodes and coding complexity

8. Conclusions

Three adaptive FEM algorithms (*h*-adaptive, *p*-adaptive and *hp*-adaptive algorithms) have been developed to solve natural convective heat transfer. Simulation results for natural convection within a differentially heated enclosure with and without a partition were obtained using the three techniques. Good agreement with data available in the literature was observed for both cases.

The computational efficiencies and requirements of the three adaptive algorithms were compared and their accuracies listed for the two heat transfer cases. For simple geometries, the *p*-adaptive scheme may be faster with regards to the CPU/DOF than the other two methods; however, the error convergence of the *hp*-adaptive technique is superior to both the *h*- and the *p*-adaptive schemes. While *hp*-adaptation may be the overall preferred choice for convective heat transfer problems, there are many problems that can be effectively solved using the more simple *h*- or *p*-adaptive schemes. Dynamically controlled adaptive FEM algorithms are especially promising in solving problems in which the characteristics of the solution are difficult to predict in advance.

References

[1] Guo, B. and Babuska, I. (1986): "The *h-p* Version of the Finite Element Method", Parts 1 and 2, *Computational Mechanics,* Vol. 1, pp. 21-21 and pp. 203-220.

[2] Gui, W. and Babuska, I. (1986): "The *h, p* and *h-p* Version of the Finite Element Method in One Dimension", Parts 1 and 2, *Numerische Mathematik* Vol. 49, pp.577-683.

[3] Wang, X. and Pepper, D. W. (To appear): "Application of an *hp*-adaptive FEM for solving thermal flow problems", *AIAA Journal of Thermophysics and Heat Transfer*.

[4] Chorin, A. J. (1968): "Numerical Solution of the Navier-Stokes Equations", *Mathematics of Computation*, Vol. 22, pp.745-762.

[5] Ramaswamy, B., Jie, T. C. and Akin, J. E. (1992): "Semi-Implicit and Explicit Finite Element Schemes for Coupled Fluid/Thermal Problems", *International Journal of Numerical Methods in Engineering,* Vol. 34, pp.675-696.

[6] Demkowicz, L, Oden, J. T., Rachowicz, W and Hardy, O. (1989): "Toward a Universal *h-p* Adaptive Finite Element Strategy, Part 1. Constrained Approximation and Data Structures", *Computer Methods in Applied Mechanics and Engineering,* Vol. 77, pp.79-112.

[7] Nithiarasu, P. and Zienkiewicz, O. C. (2000): "Adaptive mesh generation for fluid mechanics problems", *International Journal of Numerical Methods in Engineering,* 47, pp. 629-662.

[8] Zienkiewicz O. C. and Zhu R. J. Z. (1987): "A Simple Error Estimator and Adaptive Procedure for Practical Engineering Analysis", *International Journal of Numerical Methods in Engineering,* Vol. 24, pp.337-357.

[9] Oden, J. T., Demkowicz, L. Rachowicz, W. and Westermann T. A. (2000): "Toward a Universal *h-p* Adaptive Finite Element Strategy, Part 2. A Posteriori Error Estimation", *Computer Methods in Applied Mechanics and Engineering*, Vol. 77, pp.113-180.

[10] Ainsworth, M. and Oden, J. T. (2000): "*A Posteriori Error Estimation in Finite Element Analysis, Pure and Applied Mathematics"*, A Wiley-Interscience Series of Texts, Monographs and Tracts.

[11] Oden, J. T., Wu, W. and Ainsworth, M. (1995): "Three-Step *h-p* Adaptive Strategy for the Incompressible Navier-Stokes Equations, Modeling, Mesh Generation, and Adaptive Numerical Methods for Partial Differential Equations", Springer-Verlag, pp. 347-366.

[12] Pelletier, D.H., Schetz, J.A., Reddy, J.N. (1989): "Recent developments and trends in computational natural convection", *Annual Review of Numerical Fluid Mechanics and Heat Transfer*, Vol. 2, pp. 39 - 85.

[13] De Vahl Davis, G. (1983): "Natural Convection of Air in a Square Cavity: A Bench Mark Numerical Solution", International Journal of Numerical Methods in Fluids, Vol. 3, pp. 249-264.

[14] Chen, K. S, Ku, A. C. and Chou, C. H. (1990): "Investigation of Natural Convection in Partially Divided Rectangular Enclosures Both With and Without an Opening in the Partition Plate: Measurements", Journal of Heat Transfer, Vol.112, pp. 648-652.

[15] Fu, W. S and Shieh, W. J. (1998): "A Penalty Finite Element Method for Natural Convection Heat Transfer in a Partially Divided Enclosure", *International Communications of Heat and Mass Transfer*, Vol. 15, pp.323-332.